Available online at www.sciencedirect.com
SCIENCE DIRECT®
Journal of Organometallic Chemistry 686 (2003) 332–340
Journal of Organometallic Chemistry
www.elsevier.com/locate/jorganchem

Magnesium and chlorostannanes—building blocks for novel tinmodified silanes

P. Bleckmann [c], T. Brüggemann [c], S.V. Maslennikov [b,*], T. Schollmeier [c], M. Schürmann [a], I.V. Spirina [b], M.V. Tsarev [b], F. Uhlig [a,*]

[a] Institute for Inorganic Chemistry, Graz University of Technology, Stremayrgasse 16, A-8010 Graz, Austria
[b] Department of Chemistry, Nizhni Novgorod State University, Gagarin av. 23/5, Nizhni Novgorod 603950, Russia
[c] Fachbereich Chemie der Universität Dortmund, Otto-Hahn-Straße 6, D-44221 Dortmund, Germany

Received 16 May 2003; received in revised form 28 July 2003; accepted 28 July 2003

Dedicated to Prof. Dr. H. Marsmann on the occasion of his 65th birthday

Abstract

Cyclic stannasilanes with alternating Si–Sn sequences ([Ph_2Sn–Me_2Si]$_3$, **1**; [t-Bu_2Sn–Me_2Si]$_2$, **2**) were synthesized by the reaction of dimethyldichlorosilane with diorganodichlorostannanes (R_2SnCl_2, R = Ph, t-Bu) in the presence of magnesium. The reaction pathway towards **2** via the unexpected intermediate product Cl–$SiMe_2$–(t-Bu_2Sn)$_2$–$SiMe_2$–Cl (**5**) is discussed. In addition, some thermodynamic and kinetic studies for the formation of the rings (**1**, **2**) and the Grignard-type tin compounds are presented. All compounds were characterized by NMR, MS and elemental analysis. The solid state structures of **1**, **2** and **5** were determined by X-ray crystallography.

Keywords: Cyclic stannasilanes; Magnesium; X-ray crystallography

1. Introduction

Although, the chemistry of mono and polycyclic silanes and siloxanes has been well investigated during the last decades, only little is known about cyclic silanes containing elements of Groups 13, 14, or 15. In the last few years we described the syntheses of open-chain and cyclic tin-modified silanes in simple one pot synthesis by reacting dimethyl- or diphenyldichlorostannanes with diorganodichloro- or -difluorosilanes in the presence of magnesium and THF as solvent [1–4].

$$RR^1R^2Si-X+Cl-SnR^3R^4R^5 \xrightarrow[-Mg(X)Cl]{+Mg} RR^1R^2Si-SnR^3R^4R^5 \quad (1)$$

where X = Cl, F; R^1–R^4 = alkyl, aryl, silyl, stannyl; R, R^5 = halogen, alkyl, aryl.

Depending on the Si-chain length of the used α,ω-dihalodimethylsilanes (X–$(SiMe_2)_n$–X; X = F, Cl; n = 2–6) a large variety of novel monocyclic Si–Sn rings had been obtained. In continuation of this work, we reported also the synthesis of a tin and silicon containing bicyclo[2.2.2]octane (compound **F**). However, only ring sizes ranging from 6 to 8 could be obtained (**A**, n = 2; **B**, n = 3; **C**, n = 4; **D**, n = 5; **E**, n = 6; **F**, n = 4) if diphenyl- or dimethyldichlorosilanes are used as starting materials (Chart 1).

This paper is dealing with the reactions of the dimethyldichlorosilane the missing silane in the row of the Si-containing starting materials (see Chart 1) with different diorganodichlorostannanes in the presence of magnesium. The synthetic and structural investigations of the reactions and reaction pathways are accompanied by kinetic studies and theoretical calculations.

* Corresponding author.

0022-328X/03/$ - see front matter © 2003 Elsevier B.V. All rights reserved.
doi:10.1016/j.jorganchem.2003.07.001

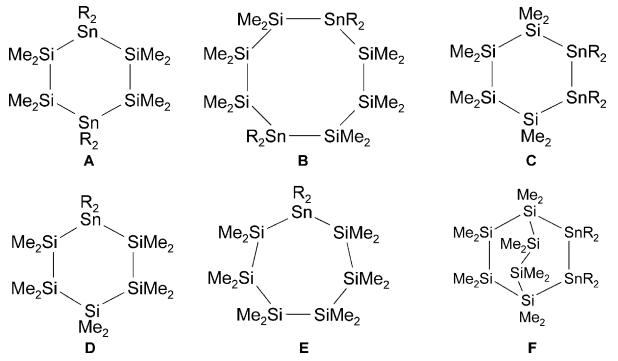

Chart 1. Reaction products of X–$(SiMe_2)_n$–X (X = F, Cl; $n = 2$–6) with R_2SnCl_2 in the presence of magnesium (**A**, $n = 2$; **B**, $n = 3$; **C**, $n = 4$; **D**, $n = 5$; **E**, $n = 6$; **F**, $n = 4$).

2. Results and discussion

2.1. Syntheses of novel tin-modified silanes

The reaction of equimolar amounts of dimethyldichlorosilane (Me_2SiCl_2) and diphenyldichlorostannane (Ph_2SnCl_2) with magnesium provided the 1,3,6-trisila-2,4,6-tristannacyclohexane (**1**) in nearly quantitative yield (Scheme 1). The four-membered 1,3-disila-2,4-distannacyclobutane (**2**) was observed by reacting Me_2SiCl_2 with the sterically more demanding di-*tert*-butyldichlorostannane in yields between 80 and 95%.

The different reaction behavior of *t*-Bu_2SnCl_2 and Ph_2SnCl_2 can be explained by the different steric demand of the substituents at the tin atoms as well as by some thermodynamic considerations.

The stability of the synthesized derivatives **1** and **2** as well as of the hypothetical compounds **3** and **4** was estimated by theoretical calculations (see Section 3.5). The calculated heats of formation are given in Chart 2. For a conversion of the six-membered ring **1** into the four-membered ring **4** a reaction enthalpie of -209.3 kJ mol^{-1} was found. The enthalpy of reaction for the transformation of compound **3** into derivative **2** was calculated with -372.5 kJ mol^{-1}. Although, these considerations are gas phase calculations, the difference

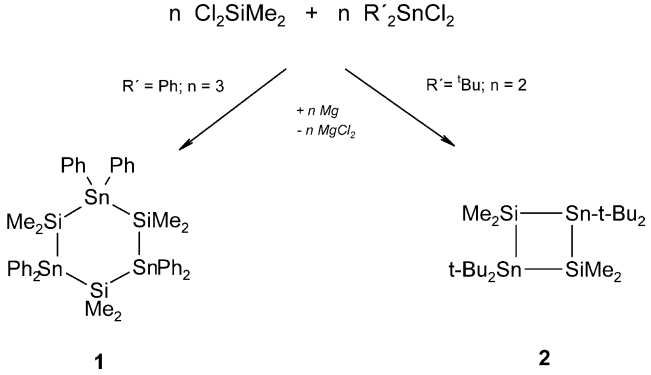

Scheme 1. Reaction of Me_2SiCl_2 with R'_2SnCl_2 (R′ = *t*-Bu, Ph) and Mg.

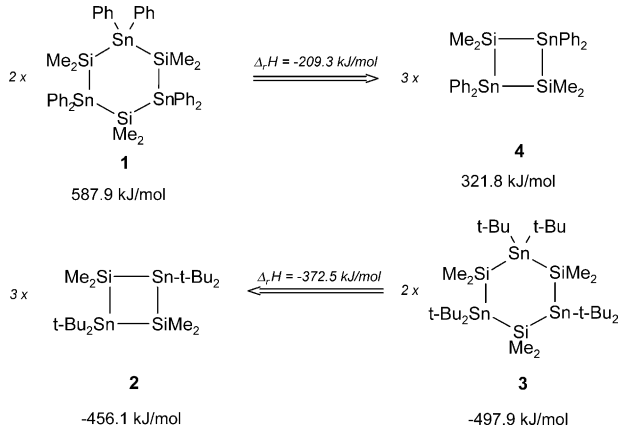

Chart 2. Heat of formation (ΔH_f) for compounds **1**, **2** and the hypothetical rings **4** and **3**. Reaction enthalpy (ΔH_r) for the conversion of **1** into **4** and **2** into derivative **3**.

in the reaction ethalpies of 163.2 kJ mol^{-1} indicates a higher stability of the four-membered *t*-butyl substituted ring **2** in comparison to the hypothetical phenyl substituted derivative **4** and display from a thermodynamical point of view the different reaction behavior of Ph_2SnCl_2 or *t*-Bu_2SnCl_2.

Surprisingly, one of the first steps in the reaction pathway towards the ring compound **2** is the formation of the distannane **5** ($ClSiMe_2$–*t*-Bu_2Sn–*t*-Bu_2Sn–$SiMe_2Cl$). This result was proven by time dependent ^{29}Si- and ^{119}Sn-NMR spectra (for ^{119}Sn-NMR see Fig. 1). The ^{119}Sn-NMR signal of the starting material at ~ 55 ppm (spectra **A**) disappeared within 1 h yielding one new singlet at -122.5 ppm for $ClSiMe_2$–*t*-Bu_2Sn–*t*-Bu_2Sn–$SiMe_2Cl$ (**5**, spectra **B**). At this stage the reaction can be stopped by quickly replacing the original solvent THF with n-hexane and we were able to isolate and characterize compound **5** by NMR and X-ray crystallography. If the solvent was not changed two new signals were observed after 3 h at -40.2 ppm (**2**), -18.2 ppm, and $+10.8$ ppm (spectra **C**). The share of the two major signal at -122.5, and -40.2 ppm changed slowly within the next 22 h (spectra **D**). After ~ 24–25 h only one major signal at -40.2 ppm (**2**) was remaining (spectra **E**), suggesting that the unidentified compounds with ^{119}Sn-NMR shifts at $+10.8$ and -18.2 ppm were intermediate products.

An identical time dependency was achieved by a series of ^{29}Si-NMR experiments. Although, there is only little experimental support for the conversion of compound **5** into the distannane **2**, we suggest that an insertion of magnesium into the tin–tin bond of derivative **5** is the key step resulting in the magnesium stannide **6** (Scheme 2). The ring closure can occur by ionic mechanism or alternatively by the intermediate formation of a silastannene ($Me_2Si{=}Sn$–*t*-Bu_2), however, the experimental data do not allow to decide between the two possible reaction pathways.

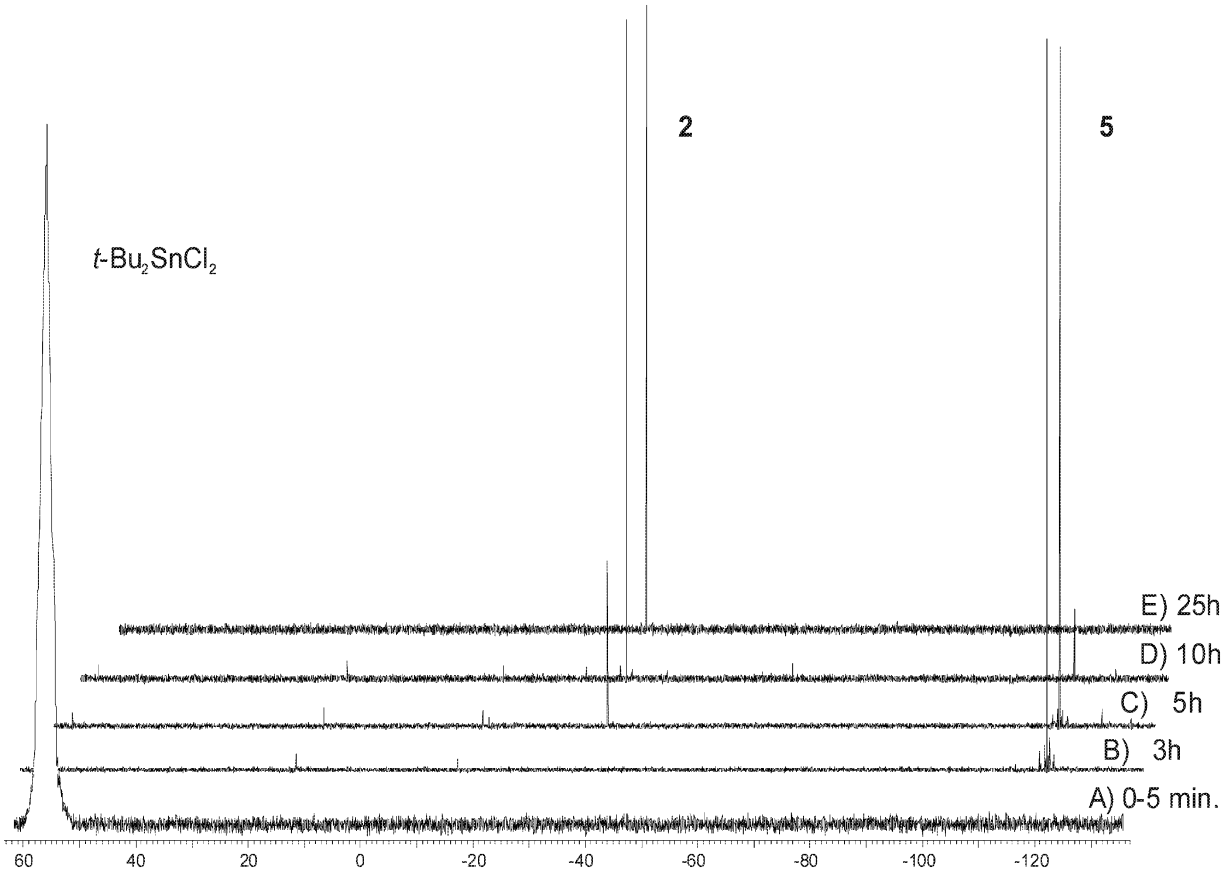

Fig. 1. Time-dependent ^{119}Sn-NMR spectra for the reaction of t-Bu_2SnCl_2, Me_2SiCl_2 and Mg. (^{119}Sn{^{1}H}-NMR: 111.91 MHz; solvent THF, D_2O-cap.; spectra A: 24 scans; spectra B–E: 1024 scans; room temperature.)

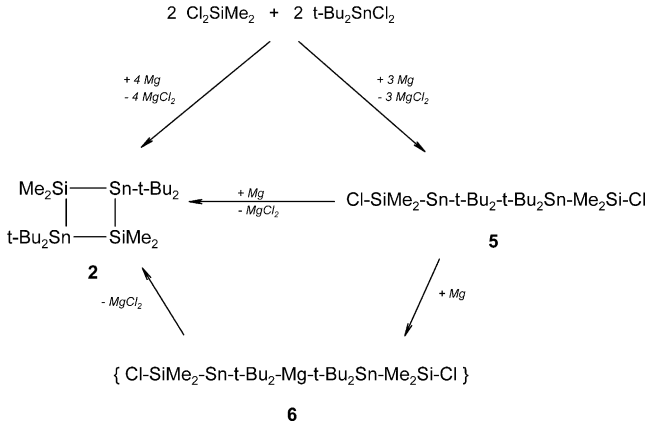

Scheme 2. Possible reaction mechanism for the formation of compound **2**.

Insertion reactions of alkaline earth metals into tin–tin bonds are well known from our own work as well as from literature (Eq. (2)) [5,6].

$$R'R_2Sn-SnR_2R' \overset{+M^{II}}{\rightarrow} R'R_2Sn-M^{II}-SnR_2R' \qquad (2)$$

where M^{II} = alkaline earth metal (Mg, Ca, Sr, Ba)

It should be carefully noted that the reaction time is highly sensitive towards small impurities of the starting materials, traces of oxygen or moisture and the concentration. Larger amounts of the solvent (THF) yielded an extended reaction time and therefore a prolonged time for the isolation of compound **5**. Although, only few examples are known in literature [7–13] we suspect that in all cases of interaction of organotin halides and organosilicon halides in the presence of magnesium, the initial step of the reactions is the formation of Grignard analogue tin compounds of type $R'_2Sn(Mg-Cl)Cl$ or $(R'R_2Sn)Mg-X$ (X = halogen, SnR_2R'). Therefore, we tried to get an independent prove for the formation of such a Grignard-type derivative. Due to the complex reaction pathway for the synthesis of compound **2**, we changed to a simpler system (Ph_2SnCl_2–Ph_3SiX–Mg) for these investigations.

2.2. Formation of Sn–Mg bonds containing intermediates

The interaction between Ph_2SnCl_2 and Ph_3SiF in the presence of Mg yielded the octaphenyl-1,3-disila-2-stannapropane ($Ph_3Si-SnPh_2-SiPh_3$). This reaction was used as a model system for studying regularities and mechanism of the formation of Si–Sn bonds. According to literature [8–10] final products of dialkyl- and diarylstannane dichlorides reduction by magnesium

are cyclic 5–7-membered polystannanes $(R_2Sn)_{5-7}$, whereas the presence of triphenylfluorosilane in the reaction leads to $Ph_3Si–SnPh_2–SiPh_3$ as major product (Eq. (3)).

$$R_2SnCl_2 + 2Ph_3SiF + 2Mg \rightarrow Ph_3Si–SnR_2SiPh_3 + 2MgClF \quad (3)$$

The formation of the Grignard analogue compounds $R_2'Sn(Mg–Cl)Cl$ and $R_2'SnSiPh_3(Mg–Cl)$ should be the key step of this reaction. In order to prove the presence of species containing a Sn–Mg bond probes were taken from the reaction mixture of Ph_2SnCl_2 with magnesium in THF at different reaction times. The solution was separated from the magnesium metal and then reacted with 1,2-dibromoethane. According to the reaction (Eq. (4)) [7] the amount of the ethylene evolved is equal to the number of Sn–Mg bonds in the solution worked up with 1,2-dibromoethane.

$$R_3SnMgCl + C_2H_4Br_2 \rightarrow R_3SnBr + MgClBr + C_2H_4 \quad (4)$$

The concentration of the Sn–Mg bonds (for $c_{Ph_2SnCl_2} = 0.25$ M l^{-1} and $T = 293$ K) was found with 0.008 mol per mol of the starting material Ph_2SnCl_2 after 40 min, 0.09 after 160 min and only traces after 400 min. The time dependence of the concentration of Sn–Mg bonds confirms their intermediate formation in the reaction.

An additional prove of the proposed formation of Sn–Mg bonds was obtained by kinetic measurements. The dependence of the reaction rate on the Ph_2SnCl_2 concentration in THF in the absence of fluorosilane is linear within the concentration range of Ph_2SnCl_2 from 0 to 0.3 mol l^{-1}. Since 0.3 mol l^{-1} is the maximal solubility of Ph_2SnCl_2 in THF, the mixture THF–toluene ($C_{THF} = 6.9$ mol l^{-1}) was used to extend the dependence to higher concentrations of the oxidizer.

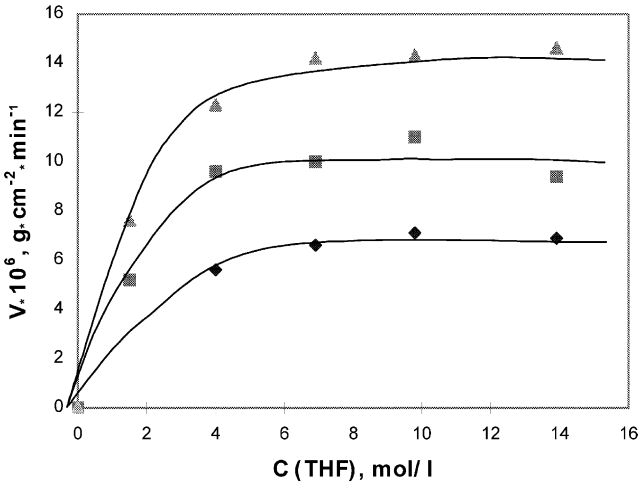

Fig. 3. The dependence of magnesium oxidation rate on THF concentration, mixture THF–toluene, C (Ph_2SnCl_2) = 0.2 mol l^{-1}. ◆, 293 K; ■, 303 K; ▲, 313 K

The rate of magnesium oxidation by Ph_2SnCl_2 in the mixture THF–toluene has a maximum at the oxidizer's concentration of 0.2 mol l^{-1}. Further increasing of the concentration of Ph_2SnCl_2 leads to a decreasing of the reaction rate (Fig. 2). The rate of the reaction vs. the concentration of THF in the mixture THF–toluene with diphenyltin dichloride concentration remaining constant is depicted at the Fig. 3.

It has been shown in literature [14] that the mechanism of a Grignard reagent formation is quite complex. On the other hand the kinetics of many reactions of metals with organic oxidizing agents (alkyl halides, metal chlorides containing organic ligands, etc.) in non-aqueous solutions can be adequately described for example by using the Langmuire–Hinshelwood or the Ealy–Redeal mechanism [15]. However, dependencies obtained for the oxidation of magnesium by diphenyltin dichloride do not correspond to any of those schemes. The closest approximation is the Langmuire–Hinshel-

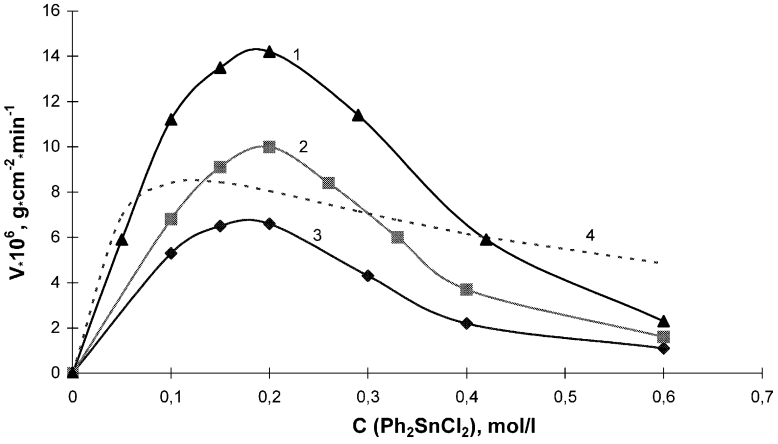

Fig. 2. The dependence of magnesium oxidation rate on Ph_2SnCl_2 concentration, mixture THF–toluene, C (THF) = 6.9 mol l^{-1}. (1) 293 K; (2) 303 K; (3) 313 K; (4) theoretical, in accordance with Eq. (8), calculated for the dependency at 303 K.

wood mechanism with the adsorption of reagents on the same reaction center.

$$R1 + S_0 \overset{K_{R1}}{\rightleftharpoons} R1S \quad (5)$$

$$R2L + S_0 \overset{K_{R2}}{\rightleftharpoons} R2S \quad (6)$$

$$R1S + R2S \overset{k}{\rightarrow} \text{products} \quad (7)$$

R1 and R2 are the reagents participating in the reaction, K_{R1} and K_{R2} are their equilibrium constants of adsorption on the metallic surface, S_0 is an active center of the metallic surface, k is the surface rate constant.

The rate of reaction is described by the expression

$$V = \frac{k*K_{R1}*K_{R2}*C_{R1}*C_{R2}}{(1 + K_{R1}*C_{R1} + K_{R2}*C_{R2})^2} \quad (8)$$

where C_{R1} and C_{R2} are reagent's concentration.

Theoretical curve obtained in accordance with Eq. (8) for the dependence at 303 K (with the adsorption equilibrium constants 112.5 for Ph_2SnCl_2 and 1.9 for THF and surface reaction rate constant 3.6×10^{-5} g cm^{-2} min^{-1}) shows the same tendency but does not repeat the experimental curve exactly (Fig. 2), especially at higher concentrations of the oxidizer. As shown above, the products of the interaction between Ph_2SnCl_2 and magnesium in the mixture THF–toluene might contain species with one or more tin-tin bonds that may be able to adsorb on the magnesium surface. It is possible that at higher Ph_2SnCl_2 concentrations such compounds with tin–tin bonds are formed, causing the discrepancies between theoretical and experimental rates of reaction. However, no experimental proof for this fact was given from the investigation of the reaction mixture.

The rate of magnesium oxidation does not depend on the amount of Ph_3SiF within the concentration range 0–0.4 mol l^{-1}. Thus, the synthesis of compounds containing bonds Si–Sn is most likely accomplished via the formation of transient organometallic species containing the Mg–Sn bond. Similar results can be observed by using Ph_3SiCl instead of the fluoro derivative.

$Ph_2Sn(MgCl)Cl$ has not been obtained as a pure compound yet. The closest analog is bis-(triphenyltin) magnesium that was observed by the reaction of magnesium with triphenyltin chloride in THF [14,16]. This compound is unstable even in the absence of oxygen and moisture and decomposes in solution by reacting with excess magnesium or THF [16]. $Ph_2Sn(MgCl)Cl$ should be even more unstable.

2.3. Structural discussion of *1*, *2* and *5*

Compounds **1**, **2** and **5** are crystalline solids and we were able to isolate these derivatives by crystallization from n-hexane. The molecular structures of **1**, **2** and **5** are presented in Figs. 4–6. Unit cell data, refinement details, and selected interatomic parameters are summarized in Tables 1 and 2.

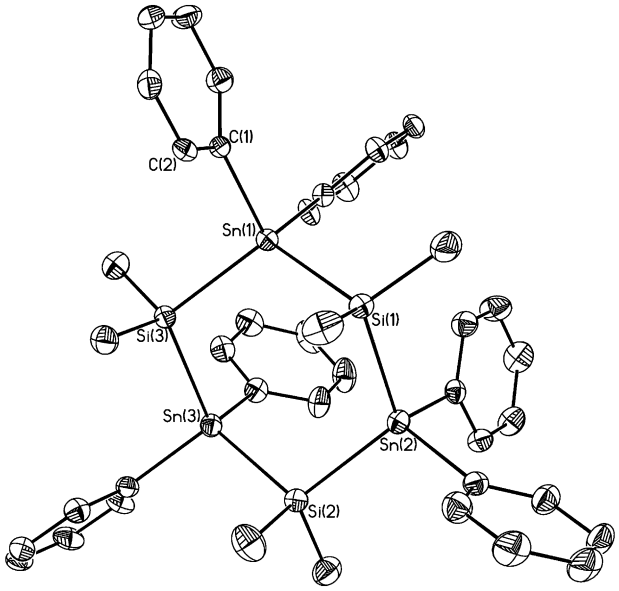

Fig. 4. View of a molecule of **1** showing 30% probability displacement ellipsoids and the atom numbering. Hydrogen atoms bonded to carbon have been removed for clarity.

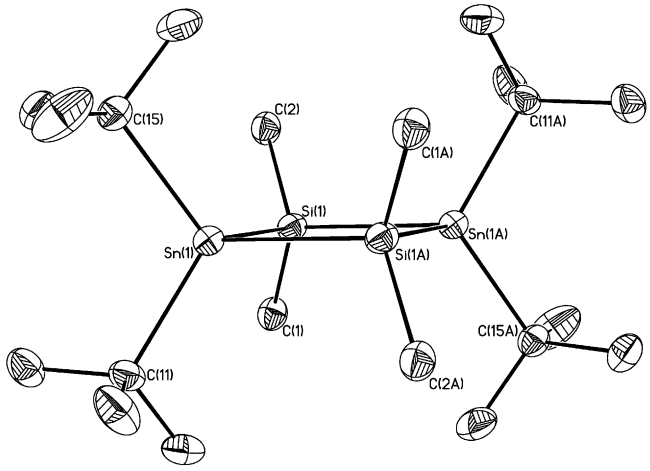

Fig. 5. View of a molecule of **2** showing 30% probability displacement ellipsoids and the atom numbering. Hydrogen atoms bonded to carbon have been removed for clarity.

2.3.1. Molecular structure of *1*

Compound **1**, depicted in Fig. 4, shows a six-membered ring comprised of an alternating Si–Sn sequence. The ring conformation is that of a classical chair resulting from the approximate tetrahedral geometry of the ring atoms. Slight distorsions from ideal tetrahedral geometry are due to the different steric demand of the ligands at the silicon and tin centers. Si–Sn–Si bond angles are observed between 113.9(5) and 115.1(9)° while Sn–Si–Sn bond angles reach from 109.7(6) up to 110.7(5)°. Silicon–tin contacts are ob-

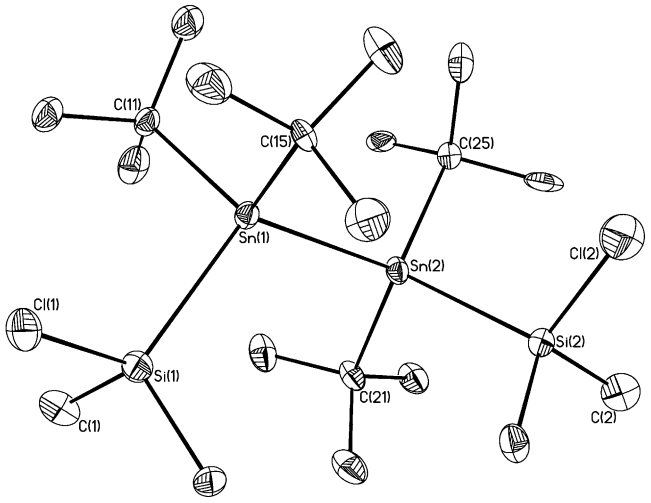

Fig. 6. View of a molecule of **5** showing 30% probability displacement ellipsoids and the atom numbering. Hydrogen atoms bonded to carbon have been removed for clarity.

served between 2.566(2) and 2.577(2) Å, and therefore in ranges observed previously in related compounds [3,4].

2.3.2. Molecular structure of 2

Compound **2**, shown in Fig. 5, crystallizes in the triclinic space group $P\bar{1}$. Due to the, in contrast to **1** higher ring strain as well as the bulkiness of the sterically more demanding *tert*-butyl groups the central Si–Sn backbone of **2** displays a nearly square planar four-membered ring with bond angles of 90.19(4)° for Si(1)–Sn(1)–Si(1A) and 89.81(4)° for Sn(1)–Si(1)–Sn(1A). The tin–Silicon distances are observed at 2.610(2) and 2.620(1) Å and therefore in ranges found in the related, less strained six-membered ring [–*t*-Bu_2Sn–$SiMe_2$–$SiMe_2$–]$_2$ [17] (2.586(3)–2.597(3) Å) as well as the five-membered ring Ph_2Si[*t*-Bu_2Sn–$SiMe_2$]$_2$ [17] (2.597(3)–2.623(3) Å). Tin–carbon distances are found at 2.207(4) and 2.208(5) Å while silicon–carbon distances are observed between 1.886(4) and 1.892(4) Å.

2.3.3. Molecular structure of 5

The distannane derivative **5** is depicted in Fig. 6. The disordered *tert*-butyl und chlorodimethylsilyl groups for compound **5** were found with occupancies of 0.2 (Si(2′), C(2′)), 0.3 (Cl(1′), Cl(2′), C(1′), C(2′)), 0.7 (Cl(1), Cl(2), C(1), C(2)) and 0.8 0.2 (Si(2), C(2)). One C atom and the Cl atom of a chlorodimethylsilyl group are disordered over two positions sharing their positions not exactly. Two pairs (Cl(1), C(1′)) and (Cl(1′), C(1)) have been refined with the same anisotropic displacement parameters (EADP [18]). At the other chlorodimethylsilyl group one C atom and the Cl atom are sharing their positions exactly (EXYZ [18]). Two pairs (Cl(2), C(2′)) and (Cl(2′), C(2)) have been refined with the same anisotropic displacement parameters (EADP [18]). Such a disorder of chloro and methyl substituents were found

Table 1
Crystal data and structure refinement for **1**, **2** and **5**

	1	**2**	**5**
Formula	C_{42} H_{48} Si_3 Sn_3	C_{20} H_{48} Si_2 Sn_2	C_{20} $H_{48}Cl_2$ Si_2 Sn_2
f_w (g mol^{-1})	993.14	582.14	653.04
Crystal system	Triclinic	Triclinic	Monoclinic
Crystal size (mm^3)	0.08 × 0.08 × 0.06	0.1 × 0.08 × 0.08	0.18 × 0.15 × 0.15
Space group	$P\bar{1}$	$P\bar{1}$	$P2_1/c$
Unit cell dimensions			
a (Å)	10.8740(3)	8.8048(7)	10.8697(1)
b (Å)	11.9251(3)	8.9379(6)	16.7084(3)
c (Å)	18.4995(6)	9.7092(9)	16.8867(4)
α (°)	73.5830(12)	78.415(5)	90
β (°)	81.5325(12)	82.359(4)	103.2599(8)
γ (°)	72.7784(13)	65.623(4)	90
V (Å^3)	2192.63(11)	680.71(9)	2985.12(9)
Z	2	1	4
ρ_{calc} (Mg m^{-3})	1.504	1.420	1.453
μ (mm^{-1})	1.804	1.924	1.937
F(000)	984	296	1320
θ Range (°)	3.04–25.36	3.42–25.31	3.03–27.46
Index ranges	$-13 \le h \le 13$, $-13 \le k \le 14$, $-21 \le l \le 22$	$-10 \le h \le 9$, $-10 \le k \le 10$, $-11 \le l \le 11$	$-14 \le h \le 14$, $-21 \le k \le 21$, $-21 \le l \le 21$
No. of reflections collected	19746	5010	27497
No. of indep refln/R_{int}	8014/0.062	2401/0.046	6799/0.038
No. of refined parameters	439	117	241
R_1 (F) ($I > 2\sigma(I)$); wR_2 (F^2) (all data) [a]	0.0372; 0.0662	0.0328; 0.0561	0.0365; 0.0784
Largest difference peak and hole (e Å^{-3})	0.921 and −0.757	0.493 and −0.532	1.019 and −0.892

[a] $R_1 = \Sigma||F_o| - |F_c||/\Sigma|F_o|$, $wR_2 = \sqrt{\Sigma\, w\{(F_o)^2 - (F_c)^2\}/\Sigma\, w\{(F_o)^2\}^2}$.

Table 2
Selected bond lengths (Å) and bond angles (°) for **1**, **2** and **5**

	1	**2**	**5**
Bond lengths			
Sn(1)–Si(1)	2.572(2)	2.610(2)	2.582(2)
Sn(1)–Si(3)	2.569(2)		
Sn(2)–Si(1)	2.577(2)		
Sn(2)–Si(2)	2.566(2)		2.547(2)
Sn(1)–Sn(2)			2.837(1)
Si(1)–Cl(1)			2.065(2)
Si(1)–Cl(2)			2.022(2)
Bond angles			
C–Sn(1)–C	104.2(2)	111.8(2)	109.63(15)
C–Sn(1)–Si(1)	107.0(1)	112.6(1)	104.12(10)
C–Sn(1)–Si(1)	110.5(1)	115.3(1)	107.08(9)
C–Sn(1)–Si	114.0(1)	113.2(1)	
C–Sn(1)–Si	106.5(1)	112.2(1)	
Si(1)–Sn(1)–Si(1)		90.19(4)	
Si(1)–Sn(1)–Si(3)	114.2(5)		
Si(1)–Sn(1)–Sn(2)			111.92(3)
C(15)–Sn(1)–Sn(2)			110.92(8)
C(11)–Sn(1)–Sn(2)			112.82(10)
C–Si(1)–C	108.2(3)	105.9(2)	107.2(8)
C–Si(1)–Sn(1)	109.9(2)	116.8(2)	114.23(13)
C–Si(1)–Sn(1)	110.2(2)	114.1(2)	114.3(8)
C–Si(1)–Sn	107.8(2)	116.5(1)	
C–Si(1)–Sn	111.0(2)	113.7(2)	
Sn(1)–Si(1)–Sn(1)		89.81(4)	
Sn(1)–Si(1)–Sn(2)	109.77(6)		
Sn(1)–Si(1)–Cl(1)			109.87(8)
C(21)–Si(1)–Cl(1)			106.97(8)
C(25)–Si(1)–Cl(1)			103.5(8)

often in organometallic chemistry mainly due to the similar radii and electron density of the groups. In addition, the tertiary carbon atoms of one *t*-butyl group and the silicon atom of a chlorodimethylsilyl group are sharing their positions exactly (EXYZ [18]), suggesting that only small energetic differences were given between the two conformers **5A** (*syn*-clinal, skew or gauche conformation) and **5B** (*anti*-periplanar, staggered conformation) in the solid state. This result is in contrast to the solid state structure of the related 1,2-dichlorotetra-*tert*-butyldistannane (t-$Bu_2Sn(Cl)$–$Sn(Cl)t$-Bu_2, **6**) for which only a trans conformer similar to **5B** was observed [19] (Chart 3).

Therefore, the two pairs (Si(2), C(25′)) and (Si(2′), C(25)) were refined with the same anisotropic displacement parameters (EADP [22]). A view along the tin–tin axis of conformer **5A** displays a distorted staggered conformation with a tin–tin distance of 2.8367(12) Å (2.8299(5) Å for **6**). The torsion angles are found between 78.69(5) and 80.50(12)° for Si(1)–Sn(1)–Sn(2)–Si(2), C(11)–Sn(1)–Sn(2)–C(21) and Si(1)–Sn(1)–Sn(2)–C(25), while the Si(1)–Sn(1)–Sn(2)–C(21), C(11)–Sn(1)–Sn(2)–C(25) and C(15)–Sn(1)–Sn(2)–Si(2) torsion angles are found around 40°.

3. Experimental

3.1. General methods

All reactions were carried out under an atmosphere of inert gas (N_2 or Ar) using Schlenk techniques. All solvents were dried by standard methods and freshly distilled prior to use. All other chemicals used as starting materials were obtained commercially. ^{1}H- and ^{13}C-NMR spectra were recorded using Bruker DRX 400 or DRX 500 spectrometer (internal reference Me_4Si). ^{29}Is- and ^{119}Sn-NMR spectra were recorded using a Bruker DRX 400 spectrometer or a Bruker DPX 300 spectrometer (internal reference Me_4Si or Me_4Sn, respectively). Mass spectra were obtained using a MAT 8200 mass spectrometer. Elemental analyses were performed on a LECO-CHNS-932 analyzer.

Chromatographic analysis of ethylene evolved in the reaction between dibromoethane and bi-organometallic compounds was performed on the chromatograph 'Tsvet-104' using 1 m glass column with activated charcoal.

3.2. Kinetic investigations

The rate of magnesium oxidation by diphenyltin dichloride was measured by controlling the electric resistance of the magnesium wire ($d = 0.5$ mm, magnesium content $> 99.9\%$) put in the reaction mixture [14]. This method was modified for performing experiments in an argon atmosphere. Before starting measurement magnesium wire was activated in the reaction cell by adding a 0.01 M solution of iodine in THF so that the change of its resistance was about 10%. Afterwards the iodine solution was removed from the reaction cell, the cell was washed with pure THF twice, and the oxidizing mixture was added.

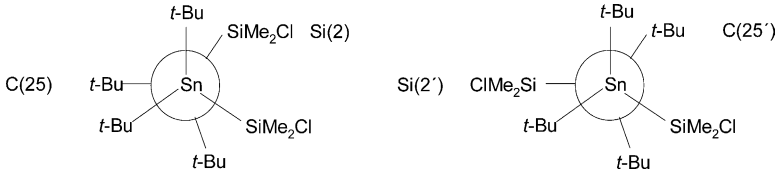

Chart 3. Conformers of compound **5** in the solid state. **5A** (*syn*-clinal, skew or gauche conformation) and **5B** (*anti*-periplanar, staggered conformation).

3.3. General procedures for **1** and **2**: the stannasilacycloalkanes **1** and **2** were prepared according to the procedures described in Ref. [3]

3.3.1. 1,1,3,3,5,5-Hexamethyl-2,2,4,4,6,6-hexaphenyl-1,3,5-trisila-2,4,6-tristannacyclohexane, [–$SiMe_2$–$SnPh_2$–]$_3$ (**1**)

Starting materials: 0.94 g (7.3 mmol) of Me_2SiCl_2, 2.5 g (7.3 mmol) of Ph_2SnCl_2, 70 ml of THF, 0.5 g (21 mmol) of Mg. The crude product was dissolved in 50 ml of *n*-hexane, and filtered (G3, with 1 cm of Celite). After removal of ~40 ml of the solvent and storage in a refrigerator (5–8 °C) 2.1 g (87%) of **1** as a colorless solid, m.p. > 250 °C, were obtained. ^{1}H-NMR (500,13 MHz, C_6D_6): δ 0.73 [$SiMe_2$, $^3J(^{119}Sn-^1H) = 33$ Hz], 7.58 [$SnPh_2$]. $^{13}C\{^1H\}$-NMR (125.77 MHz, C_6D_6): δ −0.7 [$SiMe_2$, $^2J(^{119}Sn-^{13}C) = 16$ Hz], 128.3 [$SnPh_2$-*para*], 128.9 [$SnPh_2$-*meta*, $^3J(^{119}Sn-^{13}C) = 40$ Hz], 138.6 [$SnPh_2$-*ortho*, $^2J(^{119}Sn-^{13}C) = 35$ Hz], 139.4 [$SnPh_2$-*ipso*, $^1J(^{119}Sn-^{13}C) =$ not found, $^3J(^{119}Sn-^{13}C) = 22$ Hz]. $^{29}Si\{^1H\}$-NMR (59.63 MHz, C_6D_6): δ −35.0 [$^1J(^{119}Sn-^{29}Si) = 364$ Hz]. $^{119}Sn\{^1H\}$-NMR (111.91 MHz, C_6D_6): δ −212.2 [$^1J(^{119}Sn-^{29}Si) = 361$ Hz, $^2J(^{119}Sn-^{117}Sn) = 827$ Hz]. Anal. Calc. for $C_{42}H_{48}Si_3Sn_3$ (995.01): C, 50.9; H, 4.9. Found: C, 50.4; H, 4.9%.

3.3.2. 1,1,3,3-Tetramethyl-2,2,4,4-tetra-tert-butyl-1,3-disila-2,4-distannacyclobutane, [–$SiMe_2$–Sn–*t*-Bu_2–]$_2$ (**2**)

Starting materials: 0.9 g (7 mmol) of Me_2SiCl_2, 2.0 g (6.8 mmol) of *t*-Bu_2SnCl_2, 70 ml of THF, 0.9 g (37 mmol) of Mg. Further purification follows the procedure described for compound **1** yielding 3.38 g (85%) of **2** as a colorless solid with a m.p. > 250 °C. ^{1}H-NMR (500.13 MHz, C_6D_6): δ 0.83 [$SiMe_2$, $^3J(^{119}Sn-^1H) = 26$ Hz], 1.44 [$SnCMe_3$, ($^3J^{119}Sn-^1H$) = 57 Hz]. $^{13}C\{^1H\}$-NMR (125.77 MHz, C_6D_6): δ 0.97 [$SiMe_2$, $^2J(^{119}Sn-^{13}C) = 7$ Hz], 30.2 [$SnC(CH_3)_3$, $^1J(^{119}Sn-^{13}C) =$ not found], 34.0 [$SnC(CH_3)_3$ $^2J(^{119}Sn-^{13}C) =$ not observed]. $^{29}Si\{^1H\}$-NMR (59.63 MHz, C_6D_6): δ −9.1 [$^1J(^{119}Sn-^{29}Si) = 239$ Hz]. $^{119}Sn\{^1H\}$-NMR (111.91 MHz, C_6D_6): δ −40.5 [$^1J(^{119}Sn-^{29}Si) = 239$ Hz]. Anal. Calc. for $C_{20}H_{48}Si_2Sn_2$ (582.18): C, 41.3; H, 8.3. Found: C, 40.8; H, 8.2%.

3.3.3. 1,2-bis(Dimethylchlorosilyl)-tetra-tert-butyldistannane, Cl–$SiMe_2$–*t*-Bu_2Sn–*t*-Bu_2Sn–Me_2Si–Cl (**5**)

Me_2SiCl_2 (1.0 g, 7.7 mmol), 2.3 g (7.7 mmol) *t*-Bu_2SnCl_2, and 0.5 g (37 mmol) Mg are stirred in 80 ml THF at room temperature (r.t.). After 5–10 min the mixture turned from colorless to black which indicated the start of the reaction. After 1 h the solvent was removed in vacuo and 50 ml *n*-hexane was added. The solution was filtered (G3, with 1 cm of Celite) and ~90% of the solvent was removed in vacuo. Storage of the remaining solution in a refrigerator gave 3.95 g (80%) of **5** as a colorless solid, mp (dec.): 206 °C. ^{1}H-NMR (500.13 MHz, C_6D_6): δ 0.77 [$SiMe_2$, $^3J(^{119}Sn-^1H) = 26$ Hz], 1.49 [$SnCMe_3$, $^3J(^{119}Sn-^1H) = 65$ Hz]. $^{13}C\{^1H\}$-NMR (125.77 MHz, C_6D_6): δ 8.7 [$SiMe_2$, $^2J(^{119}Sn-^{13}C) = 37$ Hz], 31.4 [$SnC(CH_3)_3$, $^1J(^{119}Sn-^{13}C) = 253$ Hz, $^2J(^{119}Sn-^{13}C) = 16.3$ Hz], 34.6 [$SnC(CH_3)_3$]. $^{29}Si\{^1H\}$-NMR (59.63 MHz, C_6D_6): δ 31.3 [$^1J(^{119}Sn-^{29}Si) = 310$ Hz, $^2J(^{119}Sn-^{29}Si) = 51$ Hz]. $^{119}Sn\{^1H\}$-NMR (111.91 MHz, C_6D_6): δ −122.8 [$^1J(^{119}Sn-^{117}Sn) = 73$ Hz]. Anal. Calc. for $C_{20}H_{48}Si_2Sn_2Cl_2$ (653.23): C, 36.8; H, 7.4. Found: C, 37.1; H, 7.5%.

3.4. Crystallography of **1**, **2** and **5**

The crystals were mounted on the diffractometer in sealed Lindemann capillaries. The data were collected at 173 K to a maximum θ of 25.36° with 323 frames for **1**, of 25.31° with 249 frames for **2** and of 27.46° with 290 frames for **5** via ω-rotation ($\Delta/\omega = 1°$) twice 10 s per frame on a Nonius Kappa CCD diffractometer using graphite monochromated Mo–K_α radiation (λ = 0.71073 Å). The structures were solved by direct methods (SHELXS-97) [20] missing atoms, were located in subsequent difference Fourier cycles and refined by full-matrix least-squares of F^2 (SHELXL-97) [21]. All non-hydrogen atoms were refined using anisotropic displacement parameters.

The H atoms were placed in geometrically calculated positions using a riding model with U_{iso} constrained at 1.2 for non-methyl and 1.5 for methyl groups times U_{eq} of the carrier C atom.

Atomic scattering factors for neutral atoms and real and imaginary dispersion terms were taken from the International Tables for X-ray Crystallography [22]. The figures were created by SHELXTL [18].

3.5. Theoretical calculations

The reaction enthalpy of a given reaction is determined by the sum of the standard heat of formation of the components. These standard heat of formation are not available directly from ab-initio calculations, therefore, the group equivalent method from Wiberg and coworkers was used [23–25]. This method describe a link between experimental determined enthalpies of formation and ab-initio energies. One of the major problems is the quantification of the ring strain in cyclic systems. However, experimental determined heats of formation are only little known for cyclic silanes or stannanes and so a model for the description of the ring strain must be used. For the description of the ring strain are a number of models known. All of them are based on the difference of energies between strained and unstrained rings [26]. With this assumption and the

known Wiberg group equivalents [27] the energies of strained cycles are calculable in comparison to those of unstrained cyclic systems to yield a correction for the strained group equivalents [27,28].

The strictness of the resulting energies of formation are within the scope of experimental limits [26,27,29]. The ab-initio calculations are based on Hartree–Fock with Stuttgarter basis set [30] by using the program package GAUSSIAN-98 [31].

4. Supplementary material

Crystallographic data for the structural analysis have been deposited with the Cambridge Crystallographic Data Centre, CCDC nos. 206079, 206078 and 206080 for compounds **1**, **2** and **5**, respectivley. Copies of this information may be obtained free of charge from The Director, CCDC, 12 Union Road, Cambridge CB2 1EZ, UK (Fax: +44-1223-336033; e-mail: deposit@ccdc.cam.ac.uk or www: http://www.ccdc.cam.ac.uk).

Acknowledgements

The authors thank funds from the Deutsche Forschungsgemeinschaft (DFG, Germany) and the Fonds der chemischen Industrie (Germany). We also acknowledge Prof. Dr. K. Jurkschat (Dortmund University) for his interest in this work.

References

[1] F. Uhlig, R. Hummeltenberg, K. Jurkschat, Phosphorus Sulfur Silicon Relat. Elem. 123 (1997) 255.
[2] F. Uhlig, C. Kayser, R. Klassen, U. Hermann, L. Brecker, M. Schürmann, K. Ruhlandt-Senge, U. Englich, Z. Naturforsch. Teil b 54 (1999) 278.
[3] C. Kayser, R. Klassen, M. Schürmann, F. Uhlig, J. Organomet. Chem. 556 (1998) 165.
[4] M. Schürmann, F. Uhlig, Organometallics 21 (2002) 986.
[5] U. Englich, K. Ruhlandt-Senge, F. Uhlig, J. Organomet. Chem. 613 (2000) 139.
[6] M. Westerhausen, Angew. Chem. Int. Ed. Engl. 33 (1994) 14.
[7] Organometallic Compounds and Radicals, Nauka, Moscow, 1985, p. 204 (in Russian).
[8] U. Blaukat, W.P. Neumann, J. Organomet. Chem. 63 (1973) 27.
[9] W.P. Neumann, J. Pedain, R. Sommer, Justus Liebigs Ann. Chem. 694 (1966) 9.
[10] B. Josseaume, N. Noiret, M. Pereyre, A. Saux, Organometallics 13 (1994) 1034.
[11] C. Tamborski, E.J. Soloski, J. Am. Chem. Soc. 83 (1961) 3734.
[12] H.J.M. Creemers, J.G. Noltes, G.J. Van der Kerk, J. Organomet. Chem. 14 (1968) 217.
[13] J.-C. Lahournere, J. Valade, J. Organomet. Chem. 22 (1970) C3.
[14] J.F. Garst, F. Ungvary, in: H.G. Richey, Jr (Ed.), Grignard Reagents—New Developments, Wiley, Chichester, 2000, p. 185.
[15] (a) S.A. Zhukov, I.P. Lavrentyev, T.A. Nifontova, React. Kinet. Catal. Lett. 4 (1974) 1105;
(b) A.V. Piskounov, S.V. Maslennikov, I.V. Spirina, V.P. Maslennikov, Appl. Organometal. Chem. 14 (2000) 570 (and references therein).
[16] G. Bremer, K.-P. Wendlandt, Introduction into Heterogeneous Catalysis (Russian ed.), Moscow, Mir, 1981, p. 48 (Russian ed.).
[17] F. Uhlig, G. Reeske, U. Hermann, M. Schürmann, Z. Anorg. Allg. Chem. 627 (2001) 453.
[18] G.M. Sheldrick, SHELXTL, Release 5.1 Software Reference Manual, Bruker AXS Inc., Madison, WI, 1997.
[19] F. Uhlig, I. Prass, U. Hermann, T. Schollmeier, U. Englich, K. Ruhlandt-Senge, J. Organomet. Chem. 646 (2002) 271.
[20] G.M. Sheldrick, Acta Crystallogr. Sect. A 46 (1990) 467.
[21] G.M. Sheldrick, SHELXL-97, University of Göttingen, Germany, 1997.
[22] International Tables for Crystallography, vol. C, Kluwer Academic Publishers, Dordrecht, 1992.
[23] K.B.J. Wiberg, Comp. Chem. 5 (1984) 197.
[24] M.R. Ibrahim, P. von Ragué Schleyer, J. Comp. Chem. 6 (1985) 157.
[25] K.B.J. Wiberg, Org. Chem. 50 (1985) 5285.
[26] K.B.J. Wiberg, Angew. Chem. 98 (1986) 312.
[27] T. Brüggemann, Diploma thesis, Dortmund University, 2000 and references therein.
[28] T. Brüggemann, P. Bleckmann, Unpublished results, 2002.
[29] M. Braunschweig, PhD thesis, Dortmund University, 2000.
[30] H. Fuentealba, H. Preuss, H. Stoll, L. v. Szentpaly, Chem. Phys. Lett. 89 (1989) 418.
[31] J.A. Pople, M.J. Frisch, G.W. Trucks, GAUSSIAN-98 Program Package, Gaussian Inc., Pittsburgh, PA, 1998.